JOURNAL OF AGRICULTURAL AND FOOD CHEMISTRY

Article

pubs.acs.org/JAFC

Investigating the Molecular Structural Features of Hulless Barley (*Hordeum vulgare* L.) in Relation to Metabolic Characteristics Using Synchrotron-Based Fourier Transform Infrared Microspectroscopy

Ling Yang,[†] David A. Christensen,[†] John J. McKinnon,[†] Aaron D. Beattie,[‡] Hangshu Xin,[†] and Peiqiang Yu[†,§,*]

[†]Department of Animal and Poultry Science and [‡]Crop Development Centre, College of Agriculture and Bioresources, University of Saskatchewan, 51 Campus Drive, Saskatoon, Saskatchewan S7N 5A8, Canada

[§]Department of Animal Science, Tianjin Agricultural University, 22 Jinjin Road, Xiqing District, Tianjin 300384, P. R. China

ABSTRACT: The synchrotron-based Fourier transform infrared microspectroscopy (SR-FTIRM) technique was used to quantify molecular structural features of the four hulless barley lines with altered carbohydrate traits [amylose, 1−40% of dry matter (DM); β-glucan, 5−10% of DM] in relation to rumen degradation kinetics, intestinal nutrient digestion, and predicted protein supply. Spectral features of β-glucan (both area and heights) in hulless barley lines showed a negative correlation with protein availability in the small intestine, including truly digested protein in the small intestine (DVE) ($r = -0.76$, $P < 0.01$; $r = -0.84$, $P < 0.01$) and total metabolizable protein (MP) ($r = -0.71$, $P < 0.05$; $r = -0.84$, $P < 0.01$). Variation in absorption intensities of total carbohydrate (CHO) was observed with negative effects on protein degradation, digestion, and potential protein supply ($P < 0.05$). Molecular structural features of CHO in hulless barley have negative effects on the supply of true protein to ruminants. The results clearly indicated the impact of the carbohydrate−protein structure and matrix.

KEYWORDS: *amylose, β-glucan, hulless and hulled barley, molecular structure, metabolic characteristics of protein, synchrotron-based infrared microspectroscopy*

INTRODUCTION

Advanced synchrotron-based Fourier transform infrared microspectroscopy (SR-FTIRM) is a nondestructive bioanalytical technique. It is capable of detecting the biomaterial structure of plant-based foods and feeds at molecular and cellular levels with the advantages of brilliant light brightness, fast data collection, higher accuracy, and small effective source size (3−10 μm).[1] SR-FTIRM is able to image the molecular chemistry of different botanical parts.[2] Several researchers applied advanced SR-FTIRM techniques to evaluate feed quality and to detect the inherent structure of plant-based feeds, such as dried distillers grains with solubles (DDGS), wheat, triticale, canola, and barley, with processing-induced and treatment-induced changes in relation to rumen degradation characteristics.[1,3−6]

Barley is superior to corn in growing in areas with a humid climate and variable precipitation (*Zea mays* L.) because barley has a lower water-holding capacity.[7] Barley grain mainly consists of a fibrous hull, pericarp, aleurone layer, endosperm, and germ.[8] Endosperm tissue is the main storage site of starch granules and, with the aleurone layer, usually accounts for the major portion of the barley kernal.[9,10] In the aleurone layer, nonstarch polysaccharides, β-glucan, and arabinoxylan are mainly found in the cell wall.[11,12] The main polymers in barley starch granules are amylose and amylopectin, which normally account for 150−250 and 750−850 g/kg of the starch, respectively.[13] Variations in starch among different cereal grains, as well as variations within cultivars, are thought to influence starch degradability in the rumen.[14−17] In feed grains, β-glucan cannot be digested by monogastric animals because of a lack of β-glucanases but can be by ruminants because of the activity of microorganisms.[18] In barley, β-glucan accounts for 20−70 g/kg of dry matter.[19] In the early 1970s, investigations of the nutritional quality of barley found the hull content of barley affected the digestible energy in monogastric animal feeding,[20] which led to the registration of some hulless barley cultivars to further extend the use of hulless barley in food, malt, and brewing.[21] New hulless barley varieties used in this project were developed by the University of Saskatchewan's Crop Development Centre with special targets for amylose and β-glucan levels. The four hulless barley lines include the following: zero-amylose type with a very high β-glucan level (CDC Fibar), a low-amylose type with a high β-glucan level (CDC Rattan), a normal-amylose type with a normal β-glucan level (CDC McGwire), and a high-amylose type with a normal β-glucan level (HB08302). The objectives of this study were (1) to apply the SR-FTIRM approach to reveal molecular structures of the four hulless barley varieties and (2) to quantify molecular structural features in relation to rumen degradation kinetics, intestinal nutrient digestion, and potential protein supply.

MATERIALS AND METHODS

Sample Preparation and Chemical Analysis. Five barley cultivars (CDC Fibar, CDC Rattan, CDC McGwire, HB08302, and CDC Copeland) were developed by the Crop Development Centre of

Received: June 17, 2013
Revised: October 14, 2013
Accepted: October 24, 2013
Published: October 24, 2013

the University of Saskatchewan and harvested at three consecutive years (2008−2010), with the exception of HB08302 (2009 and 2010). The four hulless cultivars were distinguished by their amylose and β-glucan content, while CDC Copeland hulled barley was included as a hulled control.[22] Samples were ground through a 0.5 mm screen for starch, amylose, and β-glucan analysis, and through a 1 mm screen for analysis of other chemicals. Dry matter (DM), ash, crude fat (EE), and crude protein (CP) contents were analyzed according to the procedure of the AOAC.[23] The acid detergent fiber (ADF), neutral detergent fiber (NDF), and acid detergent lignin (ADL) contents were analyzed following the procedures reported by Van Soest et al.[24] combined with the ANKOM A200 filter bag technique (ANKOM Technology Corp., Fairport, NY). The starch, amylose, and β-glucan were analyzed utilizing Megazyme test kits [catalog nos. K-TSTA, K-AMYL, and K-BGLU, respectively (Megazyme International Ltd.,Wicklow, Ireland)]. The total amount of soluble crude protein (SCP) was determined according to the procedure of Roe et al.[25] The amount of neutral detergent insoluble CP (NDICP) was determined by analyzing the NDF residues for CP,[24] while the amount of nonprotein nitrogen (NPN) was estimated by calculating the difference between the total N content and the N content in the residue after trichloroacetic acid filtration. The amount of nonstructural carbohydrate was calculated as 100 − (ash + CP + fat + NDF − NDICP), while the total amount of carbohydrate (CHO) and the amount of true protein were calculated according to the formulas of NRC Dairy 2001.[26]

Rumen Incubation and Rumen Degradation Kinetics. Rumen incubation procedures were adopted in the steps described by Yang et al.[22] Samples (1 kg) were coarsely ground through a 0.203 mm roller gap (Sven Grain Mill, Apollo Machine and Products Ltd., Saskatoon, SK) at the Chemical and Biological Engineering Laboratory of the University of Saskatchewan. Three dry Holstein cows fitted with a rumen cannula were used and tended by the guidelines of the Canadian Council on Animal Care.[27] The rumen degradation characteristics of DM, CP, starch, NDF, and CHO were determined by the *in situ* rumen incubation method.[22,28]

Degradation characteristics of DM, CP, starch, NDF, and CHO were determined using the first-order kinetic degradation model described by Ørskov and McDonald[29] and modified by Robinson et al.[30] and by Tamminga et al.[31] The results were calculated using the nonlinear (NLIN) procedure of SAS and iterative least-squares regression (Gauss−Newton method). Related parameters were calculated as described by Damiran and Yu.[32]

Intestinal Digestion of Crude Protein, Starch, and Carbohydrates. The intestinal protein digestion was estimated using the three-step *in vitro* procedure described by Calsamiglia and Stern.[33] Intestinal digestion of carbohydrate, starch, and crude protein was estimated from rumen degradation kinetics of residues after incubation as described by Calsamiglia and Stern[33] and Nuez-Ortín and Yu.[34]

Prediction of Protein Supply and Availability: DVE/OEB System and NRC Dairy 2001. The principles of the DVE/OEB system[31] and NRC Dairy 2001[26] are similar except for some differences in concepts and factors. In the DVE/OEB system, the amount of truly digested protein in the small intestine (DVE) is summarized with the truly absorbed rumen-synthesized microbial protein in the small intestine (AMCP) and the truly absorbed rumen undegraded feed protein in the small intestine (ARUP) with deduction of the endogenous protein (ENCP). OEB refers to the balance between available N and energy in the rumen.[31] A positive value indicates a potential loss of energy, while a negative value represents a shortage of N supply resulting in impaired protein synthesis.[31,35,36] In the NRC Dairy 2001 model, the amount of metabolizable protein (MP) is used to describe the protein supply. However, MP is considered to be the sum of truly absorbed rumen undegraded feed CP (ARUP), truly absorbed microbial CP (AMCP), and truly absorbed rumen endogenous protein in the small intestine (AECP).[26] Detailed calculation steps of two models followed the procedures reported by Damiran and Yu.[37]

Sample Preparation for Collection of SR-FTIRM Spectra. Five kernels of each barley variety harvested in different years were randomly selected to be cross-sectioned for analysis of endosperm tissue at the Western College of Veterinary Medicine of the University of Saskatchewan. The thin cross sections of tissues (6 μm) were unstained and mounted on barium fluoride (BaF_2) windows (Spectral Systems, Hopewell Junction, NY) using the method of Yu et al.[3]

Collection of SR-FTIRM Spectra. The SR-FTIRM experiment was performed with the IR microspectroscopy instrument coupled with synchrotron radiation from the U2B beamline at the National Synchrotron Light Source [Brookhaven National Laboratory (NSLS-BNL), Upton, NY]. Molecular spectra were collected using a Thermo Nicolet Magna 860 Step-Scan FTIR (Thermo Fisher Scientific Inc., Waltham, MA) spectrometer equipped with a Spectra Tech Continuum IR Microscope (Spectra-Tech, Inc., Shelton, CT) and mercury cadmium telluride (MCT) detector. Liquid nitrogen was added to cool the MCT detector every 8 h. The molecular structural features were determined in the mid-infrared region (∼4000−800 cm^{-1}) of the electromagnetic spectrum. Two hundred fifty-six scans were co-added to each spot to produce a high-quality IR spectrum. The spatial resolution was set at 4 cm^{-1}. The 10 spectral images from 10 randomly selected spots of each tissue endosperm window were collected in the mid-infrared region (∼4000−800 cm^{-1}) of the electromagnetic spectrum. The total number of spectral samples was 10 (spectra) × 5 (windows) × {3 (harvest years replicates) × 4 [three hulless barley (CDC Fibar, CDC Rattan, CDC McGwire) and one hulled barley cultivars (CDC Copeland)] + 2 (harvest years replicates) × 1 (HB08302)} = 700.

Univariate Analysis of Protein, β-Glucan, and Cellulosic Compounds and Carbohydrate Molecular Structure of Barley Varieties. Spectral data were analyzed by Nicolet OMNIC version 7.2 (Spectra Tech, Madison, WI). After baseline correction, the absorption peak parameters (baseline, region, peak area, and peak center height) of functional group spectral bands representing protein, β-glucan, and cellulosic compounds and carbohydrate molecular structures were recorded for univariate analysis, in which the absorption heights of protein secondary structures (α-helix and β-sheet) were identified using the second-derivative option within the protein amide I region under the same baseline of total protein area.

The absorbance bands of specific nutrients of these barley cultivars were protein amide I area (∼1768−1558 cm^{-1}) and height (∼1647 cm^{-1}), amide II area (∼1558−1475 cm^{-1}) and height (∼1542 cm^{-1}), α-helix height (∼1655 cm^{-1}), β-sheet height (∼1628 cm^{-1}), β-glucan area (∼1450−1390 cm^{-1}) and height (∼1415 cm^{-1}), cellulosic compound peak area (∼1278−1205 cm^{-1}) and height (∼1238 cm^{-1}), total carbohydrate area (CHO, ∼1195−945 cm^{-1}), and their three major CHO peak areas: first peak (∼1195−1128 cm^{-1}), second peak (∼1128−1049 cm^{-1}), and third peak (∼1049−945 cm^{-1}). Heights of these CHO peaks were collected at ∼1152, ∼1079, and ∼1024 cm^{-1}, respectively. Ratios of peak heights of protein amide I to amide II as well as ratios of α-helix to β-sheet height were also calculated.

Multivariate Molecular Spectral Analysis for SR-FTIRM Spectra. For SR-FTIRM spectral analysis, the regions of the functional group bands were separated as protein region (∼1768−1475 cm^{-1}), nonstarch CHO region (∼1475−1195 cm^{-1}), and total CHO region (∼1195−945 cm^{-1}) for multivariate molecular spectral analysis using Statistica version 8.0 (StatSoft Inc., Tulsa, OK). Agglomerative hierarchical cluster analysis (CLA) results were presented as dendograms, while principle component analysis (PCA) results were plotted on the basis of the two highest factor scores and plotted as a function of those scores.

Statistical Analysis. Because of uneven sampling of barley cultivars over the years, the experimental design for this study was a randomized incomplete block design. The statistical analyses were performed using the MIXED procedure of SAS version 9.2 (SAS Institute, Inc., Cary, NC). For nutrient profiles and absorbance intensity, the model used for the analysis was $Y_{ijk} = \mu + \rho_i + \alpha_j + e_{ijk}$; for the *in situ* rumen degradation kinetic study, intestinal digestion and nutrient prediction, the model used for analysis was $Y_{ijkl} = \mu + \rho_i + \alpha_j + \gamma_k + e_{ijkl}$, where Y_{ijkl} is an observation of the dependent variable *ijkl*, μ is the population mean for the variable, ρ_i is the effect of harvest year as a random effect, α_j is the effect of the barley cultivar as a fixed effect, γ_k is

Table 1. Effects of Altered Carbohydrate Traits on the Spectral Characteristics of Protein Amide I and II and α-Helix and β-Sheet Protein Secondary Structure in the Endosperm Region of Four Hulless Barley Varieties and One Hulled Barley Cultivar Using SR-FTIRM[a]

		hulled	hulless						
	peak region and center (cm^{-1})	CDC Copeland (n = 3)	CDC Fibar (n = 3)	CDC Rattan (n = 3)	CDC McGwire (n = 3)	HB08302 (n = 2)	SEM[b]	P value	contrast, P value (hulled vs hulless)
amylose level (% of starch)		27.0 b	2.5 d	7.7 c	25.8 b	36.9 a	0.56	<0.0001	<0.0001
amylopectin level (% of starch)		73.0 c	97.5 a	92.3 b	74.2 c	63.1 d	0.56	<0.0001	<0.0001
β-glucan level (% DM)		3.8	10.0 a	7.4 b	4.7 c	7.5 b	0.40	<0.0001	<0.0001
baseline	1768−1475								
amide I area	1768−1558	6.70 b	6.97 b	9.28 a	8.71 a	9.07 a	0.381	<0.0001	<0.0001
amide II area	1558−1475	1.33 c	1.55 bc	2.11 a	1.75 b	1.66 bc	0.154	<0.0001	<0.0001
amide I peak height	∼1647	0.10 b	0.10 b	0.13 a	0.13 a	0.13 a	0.006	<0.0001	<0.0001
amide II peak height	∼1542	0.02 b	0.03 ab	0.03 a	0.03 a	0.03 ab	0.003	0.0006	0.0011
α-helix height	∼1655	0.09 b	0.10 b	0.12 a	0.12 a	0.12 a	0.005	<0.0001	<0.0001
β-sheet height	∼1628	0.08 c	0.09 bc	0.11 a	0.10 ab	0.11 ab	0.005	<0.0001	<0.0001
area ratio of amide I to amide II		8.27	6.06	5.62	8.61	7.24	1.449	0.3579	0.3320
height ratio of α-helix to β-sheet		1.17	1.16	1.14	1.13	1.12	1.058	0.1281	0.0474

[a]Means with different letters within the same row differ (P < 0.05). Multitreatment comparison via the Tukey−Kramer method. [b]Standard error of the mean.

in situ run as a random effect, and e_{ijkl} is the random error associated with observation *ijkl*. Contrast statement was used to compare the difference between hulled and hulless barley cultivars. Means were compared using the Tukey−Kramer method, and a P < 0.05 level was considered significant.

Because the data for the correlation study were not normally distributed, rank correlations were performed using the PROC CORR of SAS with an option of SPEARMAN to quantify molecular structural features identified using SR-FTIRM techniques in relation to (1) rumen degradation kinetics, (2) intestinal nutrient digestion, and (3) prediction of protein supply to dairy cattle using the DVE/OEB system and the NRC Dairy 2001 model.

RESULTS AND DISCUSSION

Quantifying Spectral Features of Protein. Table 1 shows the absorbance peak area and height intensities of protein in the endosperm tissue of hulled and hulless barley varieties in the region of ∼1768−1475 cm^{-1}. From basic chemical analysis, amylose levels of CDC Fibar account for 2.5% of total starch while its β-glucan level was highest among barley cultivars (10.0% of DM; P < 0.05). HB08302 had the highest amylose level and a β-glucan level higher than those of CDC McGwire and CDC Copeland. Compared to hulled barley, hulless barley CDC Fibar exhibited absorbance peak intensities in terms of protein amide I and II areas, heights, and protein secondary structure heights similar to those of CDC Copeland (P > 0.05). However, they both had smaller amide I areas, shorter amide II peak heights, and shorter α-helix heights than other hulless barley varieties (P < 0.05). CDC Rattan, CDC McGwire, and HB08302 were similar with respect to most of the protein spectral features in the endosperm tissue, although CDC Rattan had a larger amide II area (2.11 IR unit) than other barley cultivars (P < 0.05). Height ratios of α-helix to β-sheet among the barley varieties ranged from 1.12 to 1.17 IR units instead of from 1.4 to 2.0 IR units for hulled barley[38] and hulless barley,[39] and there were no significant differences (P > 0.05) among barley varieties in terms of area ratios of amide I to amide II and height ratios of α-helix to β-sheet.

The CLA and PCA analyses were conducted to identify the protein structural differences among the barley cultivars in the endosperm tissue (Figure 1). Hulless barley and hulled barley varieties were not fully distinguished from each other in the protein region of 1768−1475 cm^{-1}. Upon comparison of CDC Copeland (C) to CDC Fibar (F), no clear separate cluster classes were grouped and 94.29% of the variation in protein structure between the two cultivars was explained by the first principal component (Figure 1, 1 and 2). There are overlapping areas of the two ellipses found in the PCA plot, indicating there were some similarities of protein spectral features between the two varieties. Similar results were found for hulless barley varieties upon comparison to hulless barley. With an altered amylose level with respect to that of normal amylose hulless barley, the clusters were not separated (Figure 1, 9−14). It seemed like the level of amylose increased in the starch of hulless barley; more overlapped ellipses were found in a PCA plot upon comparison to normal amylose CDC McGwire (M).

Yu[38] reported that protein secondary structures would have an influence on protein value and protein availability by affecting access to digestive enzymes. Table 2 shows the correlation between protein structural features in endosperm tissue of hulless barley and correlated parameters estimated by rumen degradation, intestinal digestion, and predicted protein supply from two models. With respect to rumen degradation of nutrients, effective degradable crude protein (EDCP) was negatively correlated to the ratio of amide I to amide II area (r = −0.66, P < 0.05), while effective degradable NDF was positively correlated to amide I area (r = 0.74, P < 0.05) and protein secondary structure (r = 0.65, r = 0.82, P < 0.05). There was no correlation found between intestinal nutrient digestion and most of the protein spectral features except a negative correlation between the ratio of amide I to amide II area and the percentage of total digestible protein in total crude protein (r = −0.75, P < 0.01) and between the ratio of protein secondary structure on absorption peak intensity and intestinal digestible bypass CHO (r = −0.61, P < 0.05). There was a

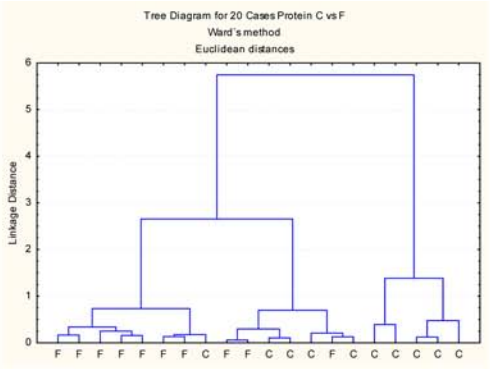

(1) CLA Comparison: CDC Copeland (C) and CDC Fibar (F)

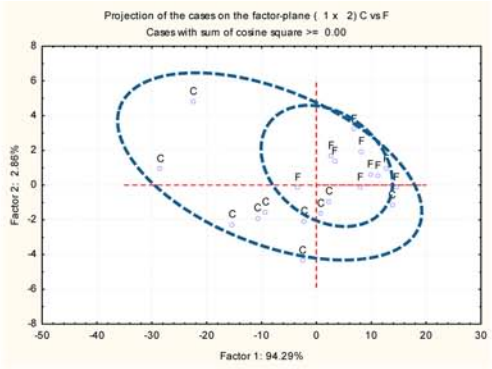

(2) PCA Comparison: CDC Copeland (C) and CDC Fibar (F)

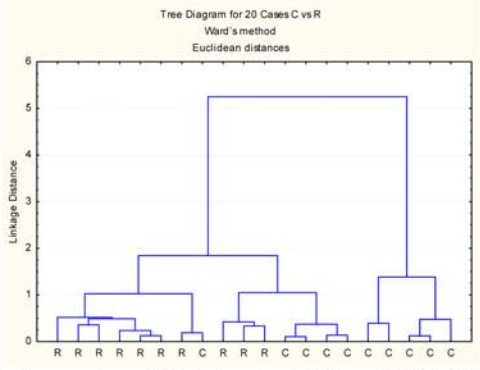

(3) CLA Comparison: CDC Copeland (C) and CDC Rattan (R)

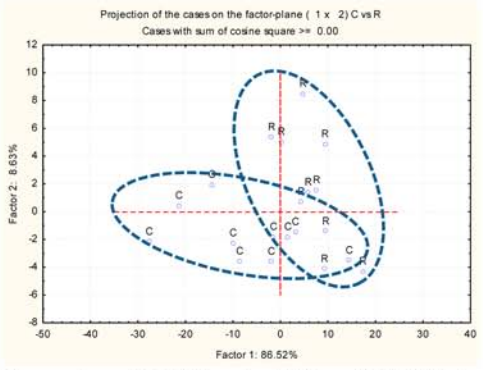

(4) PCA Comparison: CDC Copeland (C) and CDC Rattan (R)

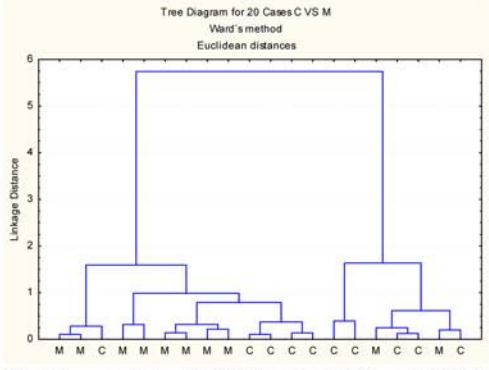

(5) CLA Comparison: CDC Copeland (C) and CDC McGwire (M)

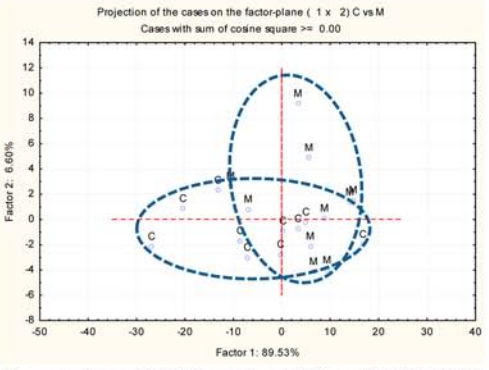

(6) PCA Comparison: CDC Copeland (C) and CDC McGwire (M)

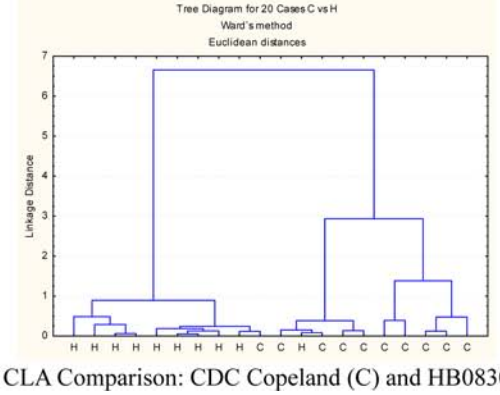

(7) CLA Comparison: CDC Copeland (C) and HB08302 (H)

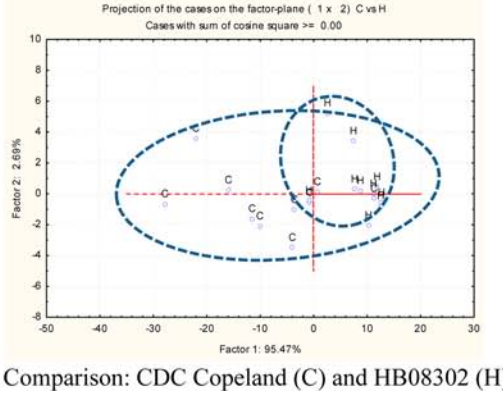

(8) PCA Comparison: CDC Copeland (C) and HB08302 (H)

Figure 1. continued

dx.doi.org/10.1021/jf403196z | J. Agric. Food Chem. 2013, 61, 11250−11260

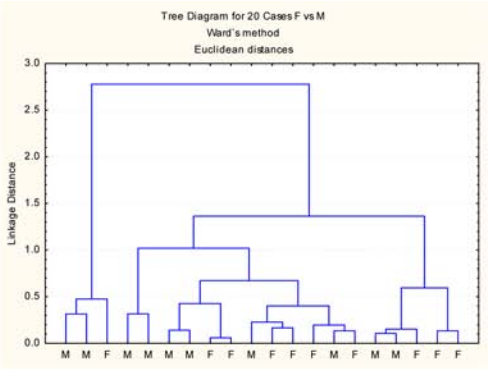

(9) CLA Comparison: CDC McGwire (M) and CDC Fibar (F)

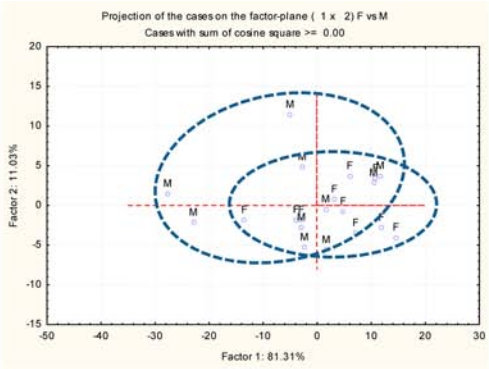

(10) PCA Comparison: CDC McGwire (M) and CDC Fibar (F)

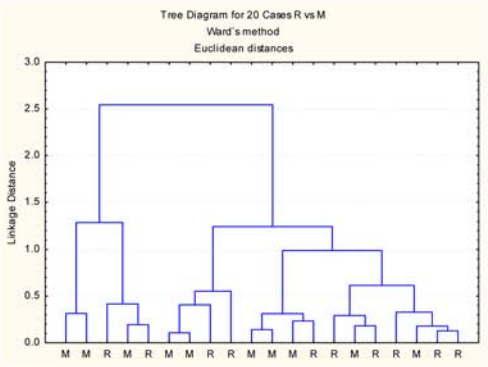

(11) CLA Comparison: CDC McGwire (M) and CDC Rattan (R)

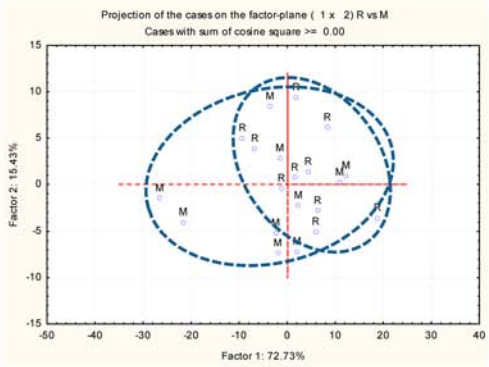

(12) PCA Comparison: CDC McGwire (M) and CDC Rattan (R)

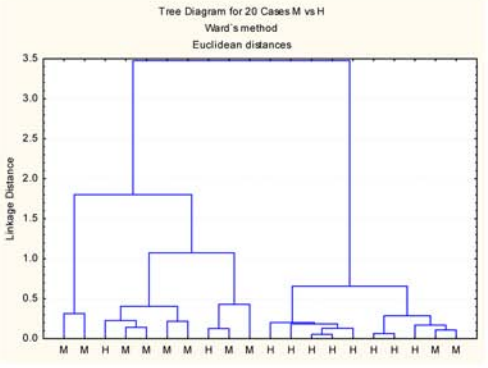

(13) CLA Comparison: CDC McGwire (M) and HB08302 (H)

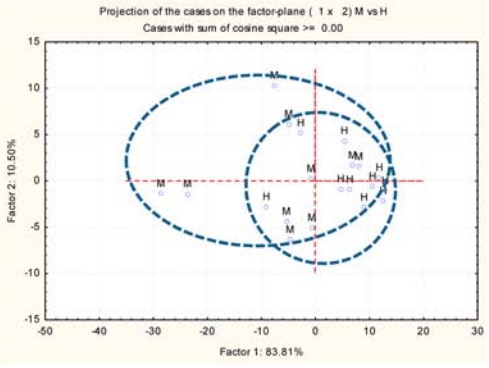

(14) PCA Comparison: CDC McGwire (M) and HB08302 (H)

Figure 1. Multivariate molecular spectral analyses of hulless barley cultivars [CDC Fibar (F), CDC Rattan (R), CDC McGwire (M), and HB08302 (H)] and a hulled barley cultivar [CDC Copeland (C)] in the SR-FTIRM protein fingerprint region (~1768−1475 cm^{-1}). CLA: (1) cluster method, Ward's algorithm; (2) distance method, Euclidean. PCA: scatter plots of the first principal components (PC1) vs the second principal components (PC2).

positive correlation between total digestible CHO and amide II peak height (r = 0.63, P < 0.05). The area ratio of amide I to amide II was negatively correlated with OEB, MCP, and AMCP (r = −0.64, P < 0.05), while MCP estimated from TDN was negatively correlated to protein spectral structure (P < 0.05).

The results suggested that protein structure differences among hulless barley cultivars might affect the availability and utilization of protein and CHO to the dairy cows, which was partially supported by the work of Damiran and Yu,[39] who reported that protein utilization was affected by protein secondary structures. The results also indicated there was a similarity in protein molecular structural makeup in endosperm tissue between CDC Fibar and hulled barley, although a significant difference between these two cultivars on protein profiles was found in chemical analysis.[22]

Quantifying Spectral Features of Nonstarch CHO (β-Glucan and Cellulosic Compounds). Table 3 shows the absorbance intensity for nonstarch CHO, including β-glucan at ~1450−1390 cm^{-1} and cellulosic compounds at ~1278−1205 cm^{-1} for barley cultivars. There was no notable difference found in β-glucan absorbance intensity among the hulless barley cultivars except for CDC Fibar (P > 0.05). Hulled barley showed a smaller β-glucan peak area (0.35 vs 0.42 IR unit, P < 0.05) and a shorter height (0.013 vs 0.016 IR unit, P < 0.05) than CDC McGwire but larger than CDC Fibar (0.35 vs 0.21 IR unit and 0.013 vs 0.009 IR unit, respectively; P < 0.05). CDC McGwire exhibited a larger peak area (0.33 IR unit) of cellulosic compound absorbance intensity than other barley cultivars (P < 0.05). CDC Fibar had the smallest peak area for cellulosic compounds (0.21, P < 0.05). There were similar peak

dx.doi.org/10.1021/jf403196z | J. Agric. Food Chem. 2013, 61, 11250−11260

Table 2. Correlation Analysis between Structural Characteristics of Protein Amide I and II and α-Helix and β-Sheet Protein Secondary Structure in the Endosperm Region (SR-FTIRM) of Four Hulless Barley Cultivars with Altered Carbohydrate Traits and Nutrient Availability and Utilization in the Rumen and Intestine[a]

	Spearman correlation *R* value							
	amide I area	amide I peak height	amide II area	amide II peak height	α-helix height	β-sheet height	ratio of amide I to amide II area	ratio of α-helix to β-sheet height
in situ rumen CP degradation								
BCP (% CP)	0.10	−0.21	−0.16	−0.34	0.05	0.03	0.66[c]	−0.44
EDCP (% CP)	−0.10	0.21	0.16	0.34	−0.05	−0.03	−0.66[c]	0.44
EDCP (g/kg of DM)	−0.22	0.03	0.30	0.06	−0.23	−0.16	−0.66[c]	0.50
in situ rumen NDF degradation								
EDNDF (g/kg of DM)	0.74[d]	0.49	0.52	0.12	0.65[c]	0.82[d]	−0.05	−0.36
intestinal CP digestion								
TDP (% CP)	−0.15	−0.17	0.14	−0.09	−0.27	−0.08	−0.75[d]	0.15
intestinal CHO digestion								
IDBCHO (% BCHO)	0.30	−0.06	−0.05	−0.16	0.24	0.18	0.56[b]	−0.61[c]
IDBCHO (g/kg of DM)	0.37	0.04	0.13	−0.08	0.30	0.26	0.43	−0.61[c]
TDCHO (g/kg of DM)	0.47	0.51	0.08	0.63[c]	0.55[b]	0.49	0.04	0.08
NRC Dairy 2001 model								
MCP_{TDN}	−0.64[c]	−0.83[d]	−0.79[d]	−0.53[b]	−0.66[c]	−0.71[c]	0.54[b]	−0.29
$AMCP^{NRC}$	−0.22	0.03	0.30	0.06	−0.23	−0.16	−0.64[c]	0.50
OEB^{NRC}	−0.22	0.03	0.30	0.06	−0.23	−0.16	−0.64[c]	0.50

[a]Abbreviations: BCP, rumen bypass crude protein; EDCP, effective degradability of crude protein; EDNDF, effective degradability of neutral detergent fiber; TDP, total digestible protein; IDBCHO, intestinal digestible bypass CHO; BCHO, rumen bypass CHO; MCP_{TDN}, microbial crude protein estimated from TDN; OEB, degraded protein balance; AMCP, truly absorbed microbial protein. [b]$P < 0.10$. [c]$P < 0.05$. [d]$P < 0.01$.

Table 3. Effects of Altered Carbohydrate Traits on the Spectral Characteristics of Nonstarch Carbohydrates (β-glucan and cellulosic compounds) in the Endosperm Region of Four Hulless Barley Cultivars and One Hulled Barley Cultivar Using SR-FTIRM[a]

		hulled	hulless						
	peak region and center (cm^{-1})	CDC Copeland (*n* = 3)	CDC Fibar (*n* = 3)	CDC Rattan (*n* = 3)	CDC McGwire (*n* = 3)	HB08302 (*n* = 2)	SEM[b]	*P* value	contrast *P* value (hulled vs hulless)
amylose level (% of starch)		27.0 b	2.5 d	7.7 c	25.8 b	36.9 a	0.56	<0.0001	<0.0001
amylopectin level (% of starch)		73.0 c	97.5 a	92.3 b	74.2 c	63.1 d	0.56	<0.0001	<0.0001
β-glucan level (% DM)		3.8 c	10.0 a	7.4 b	4.7 c	7.5 b	0.40	<0.0001	<0.0001
β-glucan									
peak area	1450−1390	0.35 b	0.21 c	0.39 ab	0.42 a	0.41 a	0.014	<0.0001	0.4291
peak height	∼1415	0.013 b	0.009 c	0.016 ab	0.016 a	0.016 ab	0.001	<0.0001	0.3486
cellulosic compounds									
peak area	1278−1205	0.26 b	0.21 c	0.28 b	0.33 a	0.28 b	0.014	<0.0001	0.2903
peak height	∼1238	0.01 b	0.01 b	0.02 ab	0.02 a	0.01 ab	0.001	<0.0001	0.1673

[a]Means with different letters within the same row differ ($P < 0.05$). Multitreatment comparison via the Tukey−Kramer method. [b]Standard error of the mean.

heights (0.01 IR unit) among barley cultivars, except for CDC McGwire ($P > 0.05$).

Although there were significant differences between barley cultivars in terms of the absorbance intensity of nonstarch CHO, the difference was not fully distinguishable from cluster classes and PCA plots within the whole nonstarch CHO region of ∼1475−1195 cm^{-1} (Figure 2). When CDC Copeland (C) was used as a control, CDC Fibar (F), the lower-amylose level hulless barley, was found to have a smaller overlapped area compared to other hulless barley varieties (Figure 2, 1−4). A significant portion of the variation (95.5%) could be explained by the first principal component between CDC Fibar and CDC Copeland (Figure 2, 1 and 2). As the level of amylose increases in hulless barley, greater similarity of spectral features in the nonstarch CHO region was found with more overlapped areas of the two ellipses from the PCA plots and mixed cluster classes

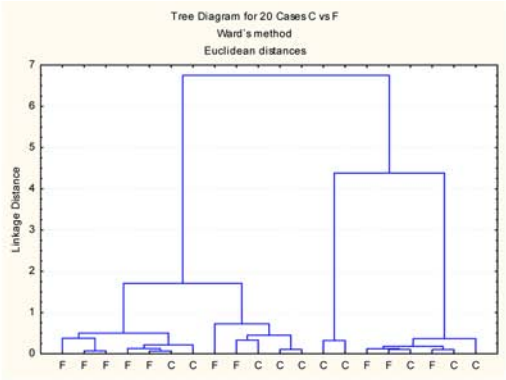

(1) CLA Comparison: CDC Copeland (C) and CDC Fibar (F)

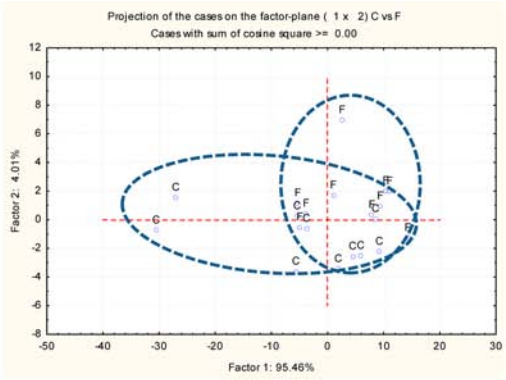

(2) PCA Comparison: CDC Copeland (C) and CDC Fibar (F)

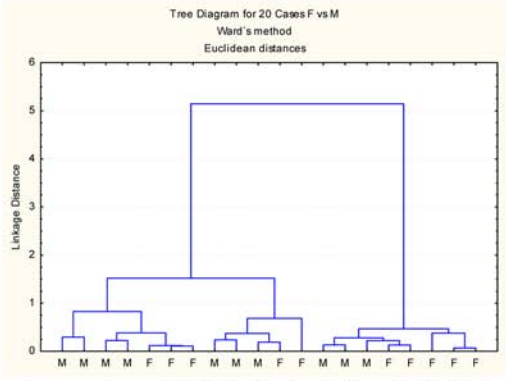

(3) CLA Comparison: CDC McGwire (M) and CDC Fibar (F)

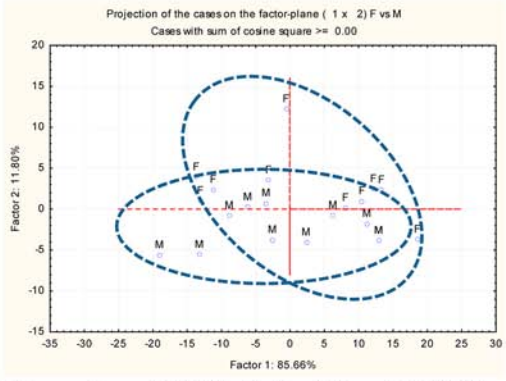

(4) PCA Comparison: CDC McGwire (M) and CDC Fibar (F)

Figure 2. Multivariate molecular spectral analyses of hulless barley CDC Fibar (F) in comparison with hulless barley CDC McGwire (M) and hulled barley CDC Copeland (C) in the SR-FTIRM nonstarch carbohydrate fingerprint region (~1475−1195 cm^{-1}). CLA: (1) cluster method, Ward's algorithm; (2) distance method, Euclidean. PCA: scatter plots of the first principal components (PC1) vs the second principal components (PC2).

($P > 0.05$). Similarly, in comparison with CDC Copeland, no fully distinguished structures were found among hulless barley cultivars in terms of nonstarch CHO ($P > 0.05$) (Figure 2, 3 and 4). Different from univariate analysis, the multivariate analysis focused on a larger nonstarch CHO area compared to the more specific β-glucan and cellulosic compound spectral regions used for univariate analysis. Therefore, there might be some other nonstarch CHO components in this region that may affect spectral features resulting in no notable structural difference from CLA clusters and PCA plots.

Because the differences in spectral characteristics of β-glucan and cellulosic compounds were found among hulless barley cultivars (Table 3), the variation of molecular structure may affect the nutritional value in terms of rumen degradation, intestinal digestion, and potential protein supply (Table 4). Correlation results between structural features of β-glucan and cellulosic compounds from FTIR and rumen digestive parameters showed significant correlations with rumen degradation kinetics and intestinal digestion of protein with cellulosic compounds in hulless barley but few correlations with β-glucan. However, spectral features of β-glucan detected by SR-FTIRM showed more significant correlation to protein and CHO metabolic characteristics than spectral features of cellulosic compounds. The peak area and height of β-glucan showed negative correlation with protein availability in rumen and small intestine, including total digestible protein (TDP, $r = -0.73$, $P < 0.05$; $r = -0.84$, $P < 0.01$) and degraded protein balance in the DVE/OEB system (OEB^{DVE}, $r = -0.61$, $P < 0.05$; $r = -0.72$, $P < 0.05$). There was a positive correlation between β-glucan peak area and total digestible CHO ($r = 0.71$, $P < 0.05$). The peak area and height of cellulosic compounds were positively correlated with effective degradable CHO (TDCHO, $r = 0.78$, $P < 0.01$; $r = 0.69$, $P < 0.05$) in the rumen as well as total digestible CHO in small intestine (TDCHO, $r = 0.85$, $P < 0.001$; $r = 0.69$, $P < 0.05$), whereas there was a negative correlation between the peak area of cellulosic compounds and truly absorbed bypass crude protein (ABCP, $r = -0.65$, $P < 0.05$) as well as metabolizable protein ($r = -0.61$, $P < 0.05$).

In normal barley, β-glucan accounts for 2−7% of the total dry matter of barley.[18,19] A higher β-glucan level may be correlated with grain ground particle size because a higher β-glucan level in the endosperm region will increase cell wall thickness, especially in the barley cell wall.[40] This may protect nutrients from rumen degradation. SR-FTIRM detects endosperm cell tissues that include structural CHO such as cellulosic compounds and nonstructural CHO like β-glucan in barley.[41−43] This could explain the more significant correlations between metabolic characteristics of crude protein and CHO and β-glucan than cellulosic compounds (Table 4), due to the fact that β-glucan is mainly located in the endosperm cell wall of barley. Hence, molecular structures of β-glucan and cellulosic compounds have an effect on the supply of protein and CHO to ruminants. The higher spectral absorption intensity of β-glucan could be associated with a lower supply of truly absorbed protein to rumen but higher total digestible CHO.

Quantifying Spectral Features of CHO. Distinct differences in absorption intensity of CHO molecular structures were observed in the comparison between hulless barley and hulled barley using univariate analyses. Table 5 shows the

Table 4. Correlation Analysis between Structural Characteristics of β-Glucan and Cellulosic Compounds in the Endosperm Region of Four Hulless Barley Cultivars with Altered Carbohydrate Traits and Nutrient Utilization and Availability in Dairy Cattle[a]

	Spearman correlation *R* value			
	β-glucan		cellulosic compounds	
	area	height	area	height
in situ rumen CHO degradation (g/kg of DM)				
EDCHO	0.57[b]	0.48	0.78[d]	0.69[c]
in situ rumen CP degradation (g/kg of DM)				
EDCP	−0.54[b]	−0.78[d]	−0.33	0.00
intestinal CP digestion				
IDP (g/kg of DM)	−0.64[c]	−0.60[b]	−0.65	−0.40
TDP (% CP)	−0.44	−0.42	−0.24	−0.17
TDP (g/kg of DM)	−0.73[c]	−0.84[d]	−0.62[c]	−0.29
intestinal CHO digestion (g/kg of DM)				
TDCHO	0.71[c]	0.60[b]	0.85[e]	0.69[c]
DVE/OEB system (g/kg of DM)				
$ABCP^{DVE}$	−0.64[c]	−0.60[b]	−0.65[c]	−0.40
DVE	−0.76[d]	−0.84[d]	−0.53[b]	−0.29
OEB^{DVE}	−0.61[c]	−0.72[c]	−0.58[b]	0.23
NRC Dairy 2001 model (g/kg of DM)				
$AMCP^{NRC}$	−0.54[b]	−0.78[d]	−0.33	0.00
MP^{NRC}	−0.71[c]	−0.84[d]	−0.61[c]	−0.23
OEB^{NRC}	−0.54[b]	−0.78[d]	−0.33	0.00

[a]Abbreviations: EDCHO, effective degradability of CHO; EDCP, effective degradability of crude protein; IDP, intestinal degradable protein; TDP, total digestible protein; TDCHO, total digestible CHO; $ABCP^{DVE}$, truly absorbed bypass protein in the small intestine; DVE, truly digested protein in the small intestine; OEB, degraded protein balance; AMCP, truly absorbed microbial protein in the small intestine; MP, metabolizable protein. [b]$P < 0.10$. [c]$P < 0.05$. [d]$P < 0.01$. [e]$P < 0.001$.

differences in spectral features of CHO in the endosperm tissue of barley cultivars in the region of ∼1195−945 cm^{-1}. Three CHO peak areas were separated in the region at ∼1195−1128, ∼1128−1049, and ∼1049−945 cm^{-1}. Among hulless barley cultivars, CDC McGwire and HB08302 had absorption areas (72.27 and 73.15 IR units, $P < 0.05$), CHO peak 2 areas (9.47 and 9.38 IR units, $P < 0.05$), CHO peak 1 heights (0.34 IR unit, $P < 0.05$), and peak 2 heights (0.47 and 0.49 IR unit, $P < 0.05$) greater than those of amylose hulless barley cultivars and also greater than those of hulled barley ($P < 0.05$).

Because of the similarity of CHO among barley cultivars in response to the IR source, SR-FTIRM failed to fully distinguish the differences in spectral features in the total CHO region of barley varieties, although the starch composition differed among hulless barley varieties. For example, with the comparison between CDC Fibar (F) and CDC Copeland (C) (Figure 3), there was no clear separation between the two clusters. The PCA plot had well-overlapped ellipses with plots representing the two cultivars, and there was only 70% variation explained by the first principal component. There was no sufficient difference detected in the whole CHO region among the barley cultivars in the endosperm tissue.

Variation in CHO absorption peak intensity among the hulless barley varieties was observed with mostly negative effects on rumen degradation, total tract digestion, and potential protein supply (Table 6). Absorption peak intensities of CHO were weakly correlated with effective degradable crude protein, protein degraded balance (in both the DVE/OEB system and the NRC Dairy 2001 model), truly absorbed microbial protein, and metabolizable protein ($P < 0.05$), intermediately strongly correlated with total digestible protein ($P < 0.01$), and strongly correlated with truly digested protein in small intestine ($P < 0.001$). This may explain the similar negative correlation results between altered starch traits (amylose and Ay:Ap ratio) and the same parameters for metabolic characteristics. The positive correlation was found only between the absorption intensity of nonstarch CHO and total digestible CHO, which was also supported by previous observation that the amylose ($r = 0.54$, $P < 0.01$) and Ay:Ap ratio were positively correlated with TDCHO ($r = 0.56$, $P <$

Table 5. Effects of Altered Carbohydrate Traits on the Spectral Characteristics of Total Carbohydrates in the Endosperm Region of Four Barley Cultivars and One Hulled Barley Cultivar Using SR-FTIRM[a]

		hulled	hulless						
	peak region and center (cm^{-1})	CDC Copeland ($n = 3$)	CDC Fibar ($n = 3$)	CDC Rattan ($n = 3$)	CDC McGwire ($n = 3$)	HB08302 ($n = 2$)	SEM[b]	*P* value	contrast *P* value (hulled vs hulless)
amylose level (% of starch)		27.0 b	2.5 d	7.7 c	25.8 b	36.9 a	0.56	<0.0001	<0.0001
amylopectin level (% of starch)		73.0 c	97.5 a	92.3 b	74.2 c	63.1 d	0.56	<0.0001	<0.0001
β-glucan level (% DM)		3.8 c	10.0 a	7.4 b	4.7 c	7.5 b	0.40	<0.0001	<0.0001
total area	1195−945	60.92 b	52.78 c	65.82 b	72.27 a	73.15 a	2.184	<0.0001	0.0056
CHO peak 1 area	1195−1128	8.31 b	5.76 c	8.28 b	9.47 a	9.38 a	0.343	<0.0001	0.7480
CHO peak 2 area	1128−1049	16.69 bc	16.5 c	18.22 bc	19.77 ab	23.28 a	0.868	<0.0001	0.0034
CHO peak 3 area	1049−945	35.95 c	30.29 d	39.03 bc	42.56 a	42.50 ab	1.215	<0.0001	0.0101
CHO peak 1 height	∼1152	0.29 b	0.20 c	0.29 b	0.34 a	0.34 a	0.012	<0.0001	0.9015
CHO peak 2 height	∼1079	0.40 bc	0.36 c	0.43 b	0.47 a	0.49 a	0.016	0.0001	0.0015
CHO peak 3 height	∼1024	0.54 c	0.44 d	0.58 bc	0.64 a	0.63 ab	0.022	0.0001	0.0332

[a]Means with different letters within the same row differ ($P < 0.05$). Multitreatment comparison via the Tukey−Kramer method. [b]Standard error of the mean.

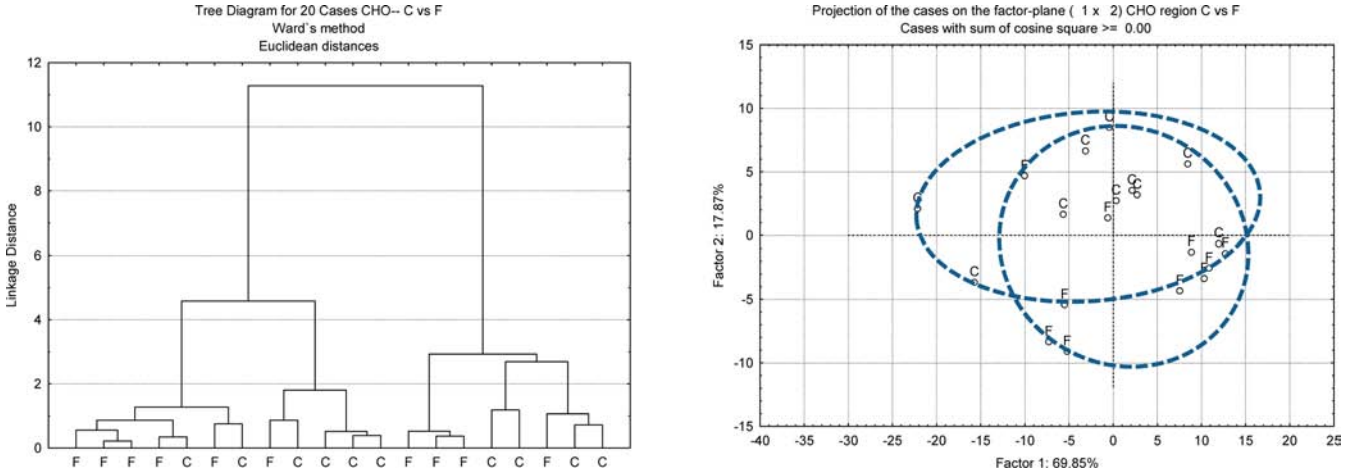

Figure 3. Multivariate molecular spectral analyses of CDC Copeland (C) compared to hulless barley CDC Fibar (F) in the SR-FTIRM carbohydrate fingerprint region (~1195–945 cm^{-1}). CLA: (1) cluster method, Ward's algorithm; (2) distance method, Euclidean. PCA: scatter plots of the first principal components (PC1) vs the second principal components (PC2).

Table 6. Correlation Analysis between Structure Spectral Characteristics of Carbohydrates in the Endosperm Region (SR-FTIRM) of Four Hulless Barley Cultivars with Altered Carbohydrate Traits and Nutrient Availability and Utilization in Dairy Cattle (in units of grams per kilogram of DM)[a]

	Spearman correlation *R* value						
	total area	CHO peak 1 area	CHO peak 2 area	CHO peak 3 area	CHO peak 1 height	CHO peak 2 height	CHO peak 3 height
in situ rumen CP degradation							
EDCP	−0.73[c]	−0.75[d]	−0.72[c]	−0.68[c]	−0.76[d]	−0.70[c]	−0.73[c]
intestinal CP digestion							
IDP	−0.64[c]	−0.61[c]	−0.52	−0.60[b]	−0.63[c]	−0.53[b]	−0.60[b]
TDP	−0.83[d]	−0.84[d]	−0.75[d]	−0.82[d]	−0.87[e]	−0.76[d]	−0.85[e]
intestinal CHO digestion							
TDCHO	0.68[c]	0.67[c]	0.55[b]	0.70[c]	0.70[c]	0.62[c]	0.70[c]
DVE/OEB system							
$ABCP^{DVE}$	−0.64[c]	−0.61[c]	−0.52	−0.60[b]	−0.63[c]	−0.53[b]	−0.60[b]
DVE	−0.91[e]	−0.92[e]	−0.88[e]	−0.89[e]	−0.91[e]	−0.90[e]	−0.92[e]
OEB^{DVE}	−0.68[c]	−0.70[c]	−0.56[b]	−0.71[c]	−0.74[d]	−0.59[b]	−0.72[c]
NRC Dairy 2001 model							
OEB^{NRC}	−0.73[c]	−0.75[d]	−0.72[c]	−0.68[c]	−0.76[d]	−0.70[c]	−0.73[c]
$AMCP^{NRC}$	−0.73[c]	−0.75[d]	−0.72[c]	−0.68[c]	−0.76[d]	−0.70[c]	−0.73[c]
MP^{NRC}	−0.72[c]	−0.71[c]	−0.65[c]	−0.67[c]	−0.73[c]	−0.67[c]	−0.69[c]

[a]Abbreviations: EDCP, effective degradability of feed crude protein; IDP, intestinal degradable protein; TDP, total digestible protein; TDCHO, total digestible CHO; ABCP, truly absorbed bypass protein in the small intestine; DVE, truly digested protein in the small intestine; OEB, degraded protein balance; MP, metabolizable protein. [b]$P < 0.10$. [c]$P < 0.05$. [d]$P < 0.01$. [e]$P < 0.001$.

0.01). Because starch and protein are the major components of endosperm tissue, spectral features of CHO in endosperm tissue were relevant to starch level in relation to nutrient availability, although there was no notable difference found by CLA and PCA among the hulless barley cultivars with altered carbohydrate composition. A possible reason for that might still be the insufficient difference detected by SR-FTIRM among barley varieties in terms of total CHO molecular structures, which included all CHO structural features instead of the one specific CHO structure such as starch. With respect to starch, the chemical structures and proportions of amylose to amylopectin are the key factors.[44] Previous studies indicated that hulless barley with lower amylose and higher β-glucan levels contained higher protein and energy levels with greater nutrient availability in the rumen and truly absorbed protein supply for postruminal digestion, as well as better synchronization of N and energy than other barley cultivars ($P <$ 0.05).[22,32,37] Via combination of barley quality for feed and nutrient availability for ruminant, hulless barley with lower amylose and higher β-glucan levels can be regarded as an alternative for ruminant feeding, although caution must be used upon addition of hulless barley to the diet due to the risk of severe acid challenge and inefficient energy utilization.

As a nondestructive method, SR-FTIRM shows the ability to detect inherent structural differences among five barley varieties. Parameters of absorption peak intensity of all detected functional group bands [protein, structure CHO (β-glucan and cellulosic compounds), and total CHO] in hulless barley cultivars were observed to have significant effects on protein, CHO, and NDF availability estimated from rumen degradation, intestinal digestion, and model predictions. This implies there are differences in the molecular structure makeup in terms of protein, nonstarch CHO, and total CHO in barley varieties, which provides a possible explanation for various metabolic

characteristics of hulless barley varieties from a molecular structure perspective. However, because of the similarities among barley CHO varities, more precise detection of specific compounds within the total CHO region may be needed to identify the possible inherent structural factors for the differences of hulless barley varieties in the total CHO region.

In conclusion, inherent structural differences of five barley varieties can be detected by SR-FTIRM in the endosperm tissue because of its brilliant light source and small aperture size. Univariate molecular spectral analysis and multivariate analysis can be applied to analyze the absorption intensity of peaks associated with functional group bands, including protein, nonstarch CHO, and total CHO. The molecular structural features of hulless barley with altered starch traits do have significant effects on the availability of protein and CHO to ruminants. Total digestible protein (TDP) and metabolizable protein (MP) were negatively affected by absorbance intensities of β-glucan and total CHO. Therefore, SR-FTIRM can be considered as an approach to identify structural molecular characteristics of cereal grain at cellular dimensions, even though more research is needed to investigate the relationship between absorption intensity of molecular structures and metabolic characteristics of nutrients at other seed layers.

AUTHOR INFORMATION

Corresponding Author

*Professor Dr. Peiqiang Yu, Ministry of Agriculture Strategic Research Chair, Department of Animal and Poultry Science, University of Saskatchewan, Room 6D10, 51 Campus Dr., Saskatoon, SK, Canada S7N 5A8. E-mail: peiqing.yu@usask.ca.

Funding

Special thanks to the Ministry of Agriculture Strategic Research Chair Program for Professor Dr. Peiqiang Yu, the Saskatchewan Agriculture Development Fund (ADF), the Natural Sciences and Engineering Research Council of Canada (NSERC) and Canada Growing Forward II for funding support.

Notes

The authors declare no competing financial interest.

ACKNOWLEDGMENTS

We appreciate the supply of the samples from the Crop Development Centre, the assistance of Z. Niu for lab work and data analysis, the kind help of L. Miller and R. Smith (NSLS-BNL) for synchrotron data collection, and guidance from all committee members and fellow authors.

ABBREVIATIONS USED

$ABCP^{DVE}$, truly absorbed bypass protein in the small intestine; ADF, acid detergent fiber; ADL, acid detergent lignin; AMCP, truly absorbed microbial protein; BCHO, rumen bypass CHO; BCP, rumen bypass crude protein; CLA, agglomerative hierarchical cluster analysis; DM, dry matter; DVE, truly digested protein in the small intestine; EDCHO, effective degradability of CHO; EDCP, effective degradability of crude protein; EDNDF, effective degradability of neutral detergent fiber; EE, ether extract (crude fat); IDBCHO, intestinal digestible bypass CHO; IDP, intestinal degradable protein; MCP_{TDN}, microbial crude protein estimated from TDN; MP, metabolizable protein; NDF, neutral detergent fiber; NDICP, neutral detergent insoluble CP; NPN, nonprotein nitrogen; OEB, degraded protein balance; PC, principal component; PCA, principal component analysis; SCP, soluble crude protein; SR-FTIRM, synchrotron-based Fourier transform infrared microspectroscopy; TDCHO, total digestible CHO; TDP, total digestible protein

REFERENCES

(1) Yu, P. Plant-based food and feed protein structure changes induced by gene-transformation, heating and bio-ethanol processing: A synchrotron-based molecular structure and nutrition research program. *Mol. Nutr. Food Res.* **2010**, *54*, 1535−1545.

(2) Wetzel, D. L.; Srivarin, P.; Finney, J. R. Revealing protein infrared spectral detail in a heterogeneous matrix dominated by starch. *Vib. Spectrosc.* **2003**, *31*, 109−114.

(3) Yu, P.; Doiron, K.; Liu, D. Shining light on the differences in molecular structural chemical make-up and the cause of distinct degradation behavior between malting- and feed-type barley using synchrotron FTIR microspectroscopy: A novel approach. *J. Agric. Food Chem.* **2008**, *56*, 3417−3426.

(4) Doiron, K. J.; Yu, P.; Christensen, C. R.; Christensen, D. A.; McKinnon, J. J. Detecting molecular changes in Vimy flaxseed protein structure using synchrotron FTIRM and DRIFT spectroscopic techniques: Structural and biochemical characterization. *Spectroscopy* **2009**, *23*, 307−322.

(5) Liu, N.; Yu, P. Characterize microchemical structure of seed endosperm within a cellular dimension among six barley varieties with distinct degradation kinetics, using ultraspatially resolved synchrotron-based infrared microspectroscopy. *J. Agric. Food Chem.* **2010**, *58*, 7801−7810.

(6) Liu, B.; McKinnon, J. J.; Thacker, P.; Yu, P. Molecular Structure and Metabolic Characteristics of the proteins and energy in triticale grains and dried distillers grains with solubles for dairy cattle. *J. Agric. Food Chem.* **2012**, *60*, 10064−10074.

(7) Thomason, W. E.; Brooks, W. S.; Griffey, C. A.; Vaughn, M. E. Hulless barley seeding rate effects on grain yield and yield components. *Crop Sci.* **2009**, *49*, 342−346.

(8) Evers, A. D.; Blakeney, A. B.; Brien, L. O. Cereal structure and composition. *Aust. J. Agric. Res.* **1999**, *50*, 629−650.

(9) Black, M. *Seed technology and its biological basis*; CRC Press: Boca Raton, FL, 2000; pp 419.

(10) Kulp, K.; Ponte, J. G. *Handbook of cereal science and technology*, 2nd ed.; Marcel Dekker: New York, 2000; pp 790.

(11) Bacic, A.; Stone, B. A. Chemistry and organization of aleirone cell wall components from wheat and barley. *Aust. J. Plant Physiol.* **1981**, *8*, 475−495.

(12) Newman, C. W.; Newman, R. K. Characteristics of the ideal barley for feed, Barley research reviews 1986−91. In *Barley Genetics VI Session and Workshops Summaries, II*; Munksgaard International Publishers: København, Denmark, 1992; pp 925−939.

(13) Ullrich, S. E.; Clancy, J. A.; Eslick, R. F.; Lance, R. β-Glucan content and viscosity of the extract from barley. *J. Cereal Sci.* **1986**, *4*, 279−285.

(14) McAllister, T. A.; Cheng, K. J. Microbial strategies in the ruminal digestion of cereal grains. *Anim. Feed Sci. Technol.* **1996**, *62*, 29−36.

(15) Mills, J. A. N.; France, J.; Dijkstra, J. A review of starch digestion in the lactating dairy cow and proposals for a mechanistic model: 1. Dietary starch characterisation and ruminal starch digestion. *Anim. Feed Sci. Technol.* **1999**, *8*, 291−340.

(16) Offner, A.; Bach, A.; Sauvant, D. Quantitative review of in situ starch degradation in the rumen. *Anim. Feed Sci. Technol.* **2003**, *106*, 81−93.

(17) Svihus, B.; Uhlen, A. K.; Harstad, O. M. Effect of starch granule structure, associated components and processing on nutritive value of cereal starch: A review. *Anim. Feed Sci. Technol.* **2005**, *122*, 303−320.

(18) Ullrich, S. E. *Barley: Production, Improvement, and Uses*; Wiley-Blackwell Publishers: Ames, IA, 2011.

(19) Zheng, G. H.; Rossnagel, B. G.; Tyler, R. T.; Bhatty, R. S. Distribution of β-glucan in the grain of hull-less barley. *Cereal Chem.* **2000**, *77*, 140−144.

(20) Bhatty, R. S.; Berdahl, J. D.; Christison, G. I. Chemical composition and digestible energy of barley. *Can. J. Animal Sci.* **1975**, *35*, 759−764.
(21) Bhatty, R. S. The potential of hull-less barley. *Cereal Chem.* **1999**, *76*, 589−599.
(22) Yang, L.; Christensen, D. A.; McKinnon, J. J.; Beattie, A. D.; Yu, P. Effect of altered carbohydrate traits in hulless barley (*Hordeum vulgare L.*) on nutrient profiles and availability and nitrogen to energy synchronization. *J. Cereal Sci.* **2013**, *58*, 182−190.
(23) *Official Methods of Analysis*, 15th ed.; Association of Official Analytical Chemists: Arlington, VA, 1990.
(24) Van Soest, P. J.; Robertson, J. B.; Lewis, B. A. Carbohydrate methodology, metabolism and nutritional implications in dairy cattle. Methods for dietary fiber, neutral detergent fiber and nonstarch polysaccharides in relation to animal nutrition. *J. Dairy Sci.* **1991**, *74*, 3583−3597.
(25) Roe, M. B.; Sniffen, C. J.; Chase, L. E. Techniques for measuring protein fractions in feedstuffs. In *Proceedings of the Cornell Nutrition Conference*; Department of Animal Science, Cornell University: Ithaca, NY, 1990; pp 81−88.
(26) National Research Council. *Nutrient Requirements of Dairy Cattle*, 7th revised ed.; National Academy Press: Washington, DC, 2001.
(27) *Guide to the Care and Use of Experimental Animals*, 2nd ed.; Canadian Council on Animal Care: Ottawa, ON, 1993; pp 212.
(28) Yu, P.; Goelema, J. O.; Tamminga, S. Using the DVE/OEB model to determine optimal conditions of pressure toasting on horse beans (*Vicia faba*) for the dairy feed industry. *Anim. Feed Sci. Technol.* **2000**, *86*, 165−176.
(29) Ørskov, E. R.; McDonald, I. The estimation of protein degradability in the rumen from incubation measurements weighted according to rate of passage. *J. Agric. Sci.* **1979**, *92*, 499−503.
(30) Robinson, P. H.; Fadel, J. G.; Tamminga, S. Evaluation of mathematical models to describe neutral detergent residue in terms of its susceptibility to degradation in the rumen. *Anim. Feed Sci. Technol.* **1986**, *15*, 249−271.
(31) Tamminga, S.; Van Straalen, W. M.; Subnel, A. P. J.; Meijer, R. G. M.; Steg, A.; Wever, C. J. G.; Block, M. C. The Dutch protein evaluation system: The DVE/OEB system. *Livest. Prod. Sci.* **1994**, *40*, 139−155.
(32) Damiran, D.; Yu, P. Chemical profile, rumen degradation kinetics, and energy value of four hull-less barley cultivars: Comparison of the zero-amylose waxy, waxy, high-amylose, and normal starch cultivars. *J. Agric. Food Chem.* **2010**, *58*, 10553−10559.
(33) Calsamiglia, S.; Stern, M. D. A three-step in vitro procedure for estimating intestinal digestion of protein in ruminants. *J. Anim. Sci.* **1995**, *73*, 1459−1465.
(34) Nuez-Ortín, W. G.; Yu, P. Estimation of ruminal and intestinal digestion profiles, hourly degradation ratio and potential nitrogen to energy synchronization of co-products of bioethanol production. *J. Sci. Food Agric.* **2010**, *90*, 2058−2067.
(35) Tamminga, S.; Jansman, A. J. M. In *Animal Nutrition*; Williams, B. A., Ed.; Wageningen Agricultural University: Wageningen, The Netherlands, 1993.
(36) Yu, P.; Christensen, D. A.; McKinnon, J. J. Comparison of the National Research Council-2001 model with the Dutch system (DVE/OEB) in the prediction of nutrient supply to dairy cows from forages. *J. Dairy Sci.* **2003**, *86*, 2178−2192.
(37) Damiran, D.; Yu, P. Metabolic characteristics in ruminants of the proteins in newly developed hull-less barley varieties with altered starch traits. *J. Cereal Sci.* **2012**, *55*, 351−360.
(38) Yu, P. Molecular chemical structure of barley protein revealed by ultra-spatially resolved synchrotron light sourced FTIR micro-spectroscopy: Comparison of barley varieties. *Biopolymers* **2007**, *85*, 308−317.
(39) Damiran, D.; Yu, P. Molecular basis of structural makeup of hulless barley in relation to rumen degradation kinetics and intestinal availability in dairy cattle: A novel approach. *J. Dairy Sci.* **2011**, *94*, 5151−5159.
(40) Oscarsson, M.; Parkkoen, T.; Auto, K.; Aman, P. Composition and microstructure of normal, waxy and high-amylose barley samples. *J. Cereal Sci.* **1997**, *26*, 259−264.
(41) Garleb, K. A.; Fahey, G. C., Jr.; Lewis, S. M. Chemical composition and digestibility of fiber fractions of certain by-product feedstuffs fed to ruminants. *J. Anim. Sci.* **1988**, *66*, 2650−2662.
(42) Garleb, K. A.; Bourquin, L. D.; Hsu, J. T.; Wagner, G. W.; Schmidt, S. J.; Fahey, G. C., Jr. Isolation and chemical analysis of nonfermented fiber fractions of oat hulls and cottonseed hulls. *J. Anim. Sci.* **1991**, *69*, 1255−1271.
(43) Gordon, A. H.; Allister, J. H.; Dinsdale, D.; Bacon, J. S. D. Polysaccharides and associated components of mesophyll cell-wall prepared from grasses. *Carbohydr. Res.* **1977**, *57*, 235−248.
(44) Song, Y.; Jane, J. Characterisation of barley starches of waxy, normal and high amilose varieties. *Carbohydr. Polym.* **2000**, *41*, 365−377.